



## OPEN ACCESS

## EDITED BY

Paolo Capuano,  
University of Salerno, Italy

## REVIEWED BY

Wenchao Chen,  
Xi'an Jiaotong University, China  
Baehyun Min,  
Ewha Womans University, Republic of  
Korea

## \*CORRESPONDENCE

Junxing Cao,  
✉ caojx@cdu.edu.cn

RECEIVED 06 December 2022

ACCEPTED 03 April 2023

PUBLISHED 19 April 2023

## CITATION

Ma S, Cao J, Liu Z, Jiang X, Su Z and Xue Y  
(2023), Gas-bearing prediction of deep  
reservoir based on DNN embeddings.  
*Front. Earth Sci.* 11:1117797.  
doi: 10.3389/feart.2023.1117797

## COPYRIGHT

© 2023 Ma, Cao, Liu, Jiang, Su and Xue.  
This is an open-access article distributed  
under the terms of the [Creative  
Commons Attribution License \(CC BY\)](#).  
The use, distribution or reproduction in  
other forums is permitted, provided the  
original author(s) and the copyright  
owner(s) are credited and that the original  
publication in this journal is cited, in  
accordance with accepted academic  
practice. No use, distribution or  
reproduction is permitted which does not  
comply with these terms.

# Gas-bearing prediction of deep reservoir based on DNN embeddings

Shuying Ma<sup>1,2,3</sup>, Junxing Cao<sup>1,3\*</sup>, Zhege Liu<sup>4,5</sup>, Xudong Jiang<sup>1,3</sup>,  
Zhaodong Su<sup>1,3</sup> and Yajue Xue<sup>4,5</sup>

<sup>1</sup>State Key Laboratory of Oil and Gas Reservoir Geology and Exploitation, Chengdu University of Technology, Chengdu, Sichuan, China, <sup>2</sup>School of Network & Communication Engineering, Chengdu Technological University, Chengdu, China, <sup>3</sup>College of Geophysics, Chengdu University of Technology, Chengdu, Sichuan, China, <sup>4</sup>Sichuan Provincial Key University Laboratory of Meteorological Information and Signal Processing, Chengdu University of Information Technology, Chengdu, China, <sup>5</sup>College of Communication Engineering, Chengdu University of Information Technology, Chengdu, China

The extraction of gas-bearing information from the deeply underground reservoir is extremely difficult due to the weak seismic response and complicated gas distribution characteristics. To predict gas-bearing reservoirs efficiently, we developed a deep neural network (DNN) embedding-based gas-bearing prediction scheme. First, the cepstrum coefficient that is sensitive to hydrocarbons is computed using the raw seismic data. A DNN model inspired by the x-vector in speech recognition is designed, comprising the long short-term memory (LSTM) networks and two fully connected (FC) networks, stacked from the bottom to the top layer. Then, the cepstrum features are fed into the DNN for training and testing, and DNN embedding is extracted from the top layers after optimized network parameters are determined. Finally, the gas-bearing probability of the reservoir is predicted by calculating the cosine distance between pairs of DNN embeddings. When applied to synthetic seismic data, the proposed method offers greater than 90% accuracy at SNR > 3 dB. Besides, the predicted result applied in deep carbonate reservoirs in China's Sichuan Basin is in basic agreement with the actual situation, demonstrating the certain feasibility of the proposed scheme.

## KEYWORDS

gas-bearing prediction, DNN embedding, TDNN, LSTM, cepstrum, deep reservoirs

## 1 Introduction

The targets for oil and gas exploration continue to develop to greater depths as the conventional technology for exploration in the petroleum industry advances. Deeply underground reservoirs are covered by massive thick sediments that have minimal physical differences from surrounding rocks, low porosity, strong non-homogeneity, and poor seismic response, making the distribution of oil and gas complicated. Traditional methods used to detect gas-bearing properties in reserves include the “bright spot” method (Hammond, 1974), AVO analysis (Hampson, 1991), and low-frequency shadowing (Taner et al., 1979). These methods are effective in specific scenarios (Cao et al., 2022), for example, bright spot technology is mainly useful in shallow unconsolidated clastic reservoirs, while AVO analysis technology is suitable for formations with a relatively simple and gentle structure. Low-frequency shadowing is mainly applied to lithologies that are already known. However, these traditional techniques are difficult to effectively quantify the complex and

non-linear connection between seismic response and gas-bearing properties in deeply buried reservoirs.

Recently data-driven deep learning methods are widely used in geophysics for first-to-wave pickup (Liao et al., 2020; Qu et al., 2021), seismic data denoising (Wang and Chen, 2019; Liu et al., 2020; Liu et al., 2022), and seismic facies recognition (Tschannen et al., 2020; Liu et al., 2021). Due to the advantage of automatically characterizing complex multivariate non-linear relationships, DNN is also used for acquiring reservoir gas-bearing properties. For example, a deep neural network (DNN) model with several hidden layers (Yang et al., 2021; Zhang et al., 2022) is built for gas-bearing prediction by leveraging the capability of DNN to handle an end-to-end task. The convolution neural network (CNN), one of the most promising DNN approaches for geophysics issues, has been trained for extracting oil and gas properties (Song et al., 2022). The characteristics of the reservoir are reflected in the comparison with the surrounding rock layers above and below it. However, these methods primarily concentrate on learning the gas-bearing information of the target layer, and the contextual relationship between the seismic waveforms is not given the same level of attention.

Although there have been many deep learning methods applied to the processing and interpretation of seismic data, few studies have focused on hydrocarbon detection. This article presents an innovative experiment that uses neural networks to quantitatively identify the gas-bearing information in seismic records based on the similarities between seismic and acoustic data. The similarities are manifested in two aspects (Xie et al., 2017). First, seismic primary waves and acoustic waves can be considered as the same kind of wave since their propagation in the elastic medium follows the same physical laws. In addition, both can be characterized by convolutional models. The seismic record can be seen as a convolution of stratigraphic reflection coefficients and waves, and the acoustic record can be regarded as the convolution of the vocal cord excitation and the vocal tract. Therefore, speech feature parameters can be integrated into seismic data processing. For example, cepstrum is applied to the computation for thin beds thickness (Hall, 2006) and gas-bearing detection (Tian and Cao, 2011; Xue et al., 2016), and the Linear Prediction cepstral Coefficient (LPCC) is utilized for seismic facies analysis (Xie et al., 2016). With the demand for improving speaker

recognition technology, the novel speech characteristics generated by DNN have grown increasingly prominent. Especially, the x-vector, namely, DNN embedding, captures accurately the vocal information of speakers by translating arbitrary-length inputs into fixed-length embeddings, making it effective for short-time records (Snyder et al., 2017; Snyder et al., 2018). Therefore, this article utilizes DNN embedding to predict gas-bearing reservoirs due to its outstanding feature extraction ability for short seismic responses.

Facing the problems of weak seismic response and thin thickness of deep buried reservoirs, we have improved and modified the DNN model prediction method. First of all, for data preparation, we obtained datasets tailored to seismic data characteristics. And the cepstrum is employed as the DNN input since it has been shown sensitive to the response of the gas-bearing layer (Cao et al., 2011; Cao et al., 2019). Secondly, in terms of the DNN model, it employed long short-term memory (LSTM) networks as the bottom layer to contextualize feature learning and the two FC layer as the primary top layer for embedding extraction. Thirdly, to visualize the gas-bearing distribution, the backend of the model outputs DNN embedding pairs' similarity using cosine distance. Evaluations based on both synthetic and actual seismic records from China's Sichuan Basin demonstrate that our method has significant advantages over traditional SVM-based approach (Tian and Cao, 2011).

## 2 Materials and methods

Since acoustic waves and seismic waves share certain similarities described above, it is theoretically possible to apply speaker recognition technology to identify certain geological bodies, such as gas-bearing reservoirs. Speaker recognition identifies the speaker by acquiring common features in numerous utterances. Similarly, when common characteristics in seismic records are extracted for gas-bearing prediction, the gas-bearing reservoir corresponds to the speaker, and the seismic records correspond to the acoustic records. Nonetheless, these two records differ, and the technique cannot be transferred directly. Based on the characteristics of the seismic data, the proposed scheme displayed in Figure 1 is designed for seismic records.

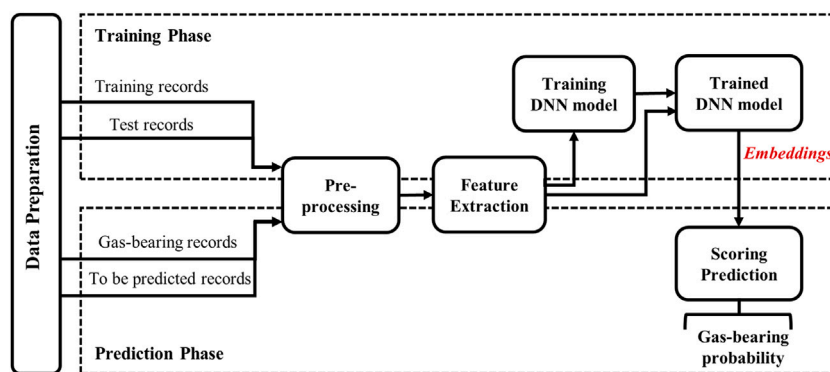


FIGURE 1 Workflow of gas-bearing prediction for the deep reservoir based on DNN Embeddings.

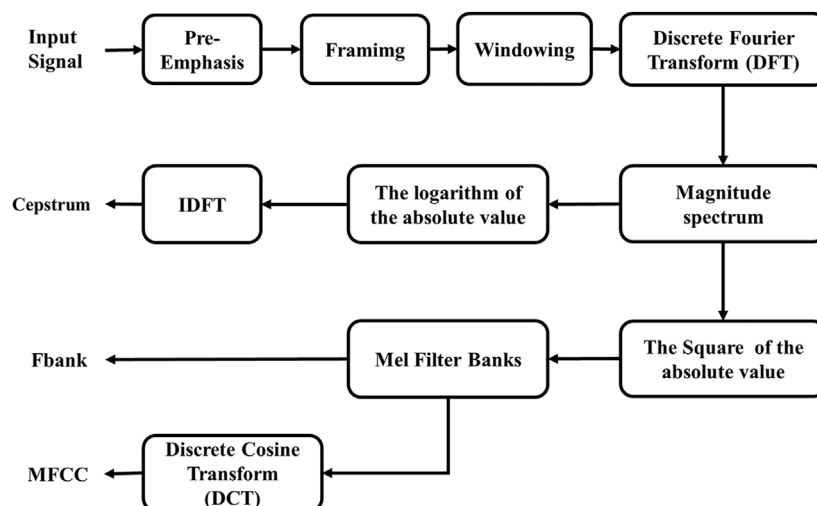


FIGURE 2  
The extraction process of MFCC, FBank, and Cepstrum features.

## 2.1 Data preparation

When preparing the dataset, the difference in attenuation, repeatability, and frequency of seismic data must be taken into consideration (Cao et al., 2011; Cao et al., 2019).

### 2.1.1 Attenuation

The speaker is the source of speech records, and there is no attenuation as time passes. While the source of seismic records is the reflection or dispersion of the seismic source signal, which is a secondary source and decays with increasing recording time. Therefore, amplitude-preserving processing is necessary (Gao et al., 2022) to remove the effects of spherical diffusion and inelastic attenuation.

### 2.1.2 Repeatability

The “voiceprint” characteristic is repeated in a single utterance for acoustic records, and a single speaker can give numerous bits of utterances. Seismic records are continuous and redundant (Coléou et al., 2003). The continuity means that the geological condition over a certain spatial range is similar, which is the foundation of tectonic and stratigraphic interpretation. The redundancy exists in some spreading information of wavefront propagation that occurs in both longitudinal and lateral directions. To sum up, seismic records within a certain lateral and longitudinal range can be approximately regarded as the response of a similar reservoir.

### 2.1.3 Short-time smoothness

Speech recognition decomposes acoustic records into frames, and each frame can be regarded as a smooth signal. The frequency of seismic records is much lower than the frequency of acoustic records, so the seismic response can only be considered smooth when the time window is narrow. Since the characteristics of the reservoir are reflected in the comparison with the surrounding rock above and below it, the window can be expanded within a reasonable range.

## 2.2 Pre-processing

Before extracting the features from the raw seismic records, pre-processing needs to be implemented. Pre-processing consists of pre-emphasis, framing, and windowing operations. Except for important parameter values which are specially set according to our practical experience, the process is consistent with speech signal processing (Muda et al., 2010).

## 2.3 Feature extraction

The cepstrum feature is selected as the input feature for DNN to extract stratigraphic response features by taking into account the following factors. Firstly, the cepstrum feature is sensitive to gas-bearing characteristics in hydrocarbon prediction (Cao et al., 2011; Cao et al., 2019). Then, the cepstrum has a simple derivation process compared with the widely used Mel Frequency Cepstral Coefficient (MFCC) and the FilterBank (FBank) (Zheng et al., 2001; Wang et al., 2014) in speech recognition, which is represented in Figure 2. Moreover, the cepstrum also can simplify the relation between seismic wavelet and stratigraphic reflection coefficients which will be demonstrated below.

The cepstrum is the real component of the Inverse Discrete Fourier transform (IDFT) for a time domain sequence’s logarithmic amplitude spectrum, which is a homomorphic transform. Assume that  $[x(n), n = 0, 1, 2, \dots, N - 1]$  is a time domain discrete signal with  $N$  sampling points, in which  $n$  is the discrete sampling of time. The cepstrum of  $x(n)$  is described by the equation below.

$$\overline{x(n)} = \text{Re}[F^{-1}(\log|F(x(n))|)] \quad (1)$$

In the Formula 1,  $F$  denotes Discrete Fourier transform (DFT),  $F^{-1}$  denotes IDFT, and  $|\cdot|$  denotes the mode-taking operation. Besides,  $F(x(n))$  can be written as  $X(k)$ , in which  $X(\cdot)$  represents the frequency domain signal of  $x(n)$  and  $[k = 0, 1, 2, \dots, N - 1]$  is the discrete sampling of the analog frequency.

The discrete seismic signal is expressed as the following equation based on the seismic record convolutional model.

$$s(n) = w(n)*r(n) \tag{2}$$

In Formula 2,  $r(n)$  is the stratigraphic reflection coefficient,  $w(n)$  is the seismic wavelet, which is typically the Ricker wavelet, and  $*$  is the convolution operation. According to Formula 1, the cepstrum domain parameters of the seismic record can be computed as follows.

$$Re[F^{-1}(\log|S(k)|)] = Re[F^{-1}(\log|W(k)|)] + Re[F^{-1}(\log|R(k)|)] \tag{3}$$

In Formula 3,  $S(k)$ ,  $W(k)$  and  $R(k)$  are the spectrum of seismic record, seismic wavelet, and reflection coefficients, respectively. In the cepstrum domain, the correlation between seismic wavelet and reflection coefficient becomes simple, i.e., the convolutional relationship in the time domain becomes a sum of two in the cepstrum. Before input to DNN, the energy, mean, and variance of the cepstrum are added to the first three dimensions of each frame feature to enhance the dimensionality of the feature parameters.

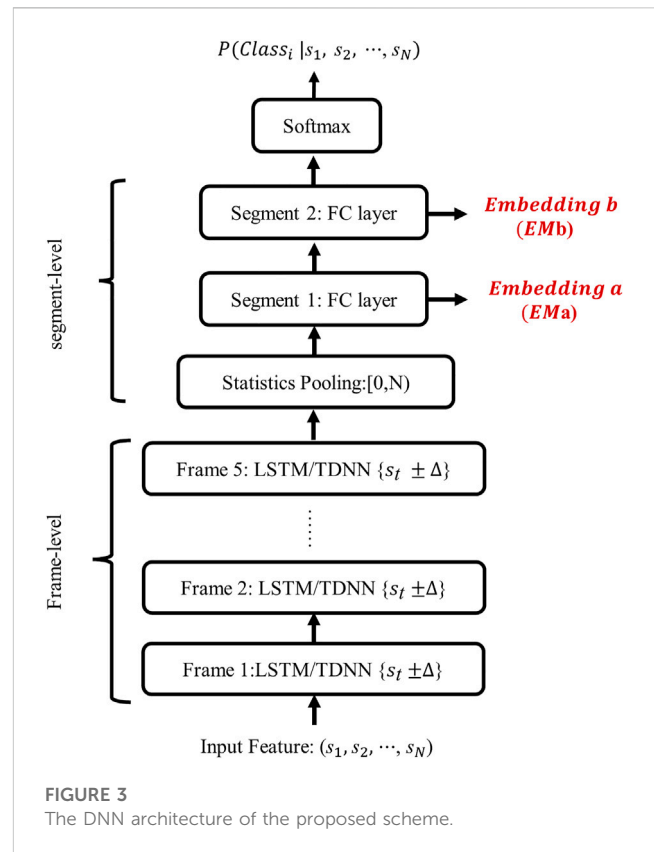
### 2.4 Training DNN model

The DNN architecture is comparable to the network architecture in the Kaldi Voxceleb recipe (Kumar et al., 2020), which consists of the frame-level layer, segment-level layer, and softmax layer as shown in Figure 3. The first frame-level layers in Kaldi consist of time-delay neural networks (TDNN) with a context and are utilized for learning repetitive features in multiple frames. In this paper, we suggest switching from TDNN to LSTM networks, because that LSTM can automatically learn long-term relationships between sequences and have a similar time-delay function. And then, the segment-level layer gathers information from the context to recognize the segment characteristics of seismic records, among which, a statistical pooling layer combines the mean and standard deviation from the output of frame 5, and two fully connected (FC) layers can be utilized to extract embedding after the training is completed. The number of hidden layer nodes is reduced according to the length of the frame there because of the smaller size of seismic data. The top softmax layer outputs the maximum posterior probability for each reservoir type and it is no longer required once the DNN training is complete. In addition, each layer has a batch normalization (BN) layer and a rectified linear units (ReLU) activation function to enhance DNN performance.

### 2.5 Scoring prediction

The front of our proposed method is used for extracting seismic embeddings. Once the DNN model has been trained, two FC layers produce the embeddings, which are the representations of the seismic records. The output of segment 1 is Embedding a (EMa), which is immediately output on the statistics layer, while the output of segment 2 is Embedding b (EMb), which is extracted from the FC layer after the ReLUs layer.

The back-end in our scheme is scoring prediction based on the embedding similarity. The embedding of the gas reserve is derived



from the seismic record adjacent to the gas-bearing well, which is indicated as  $EM_g$ . Similarly, the embedding for a seismic record to be predicted is labeled as  $EM_p$ . The embedding similarity between  $EM_g$  and  $EM_p$  represents the gas-bearing probability of the corresponding layer where the seismic records are located. The normalized cosine distance is employed in this research to represent the similarity, which is described by the equation below.

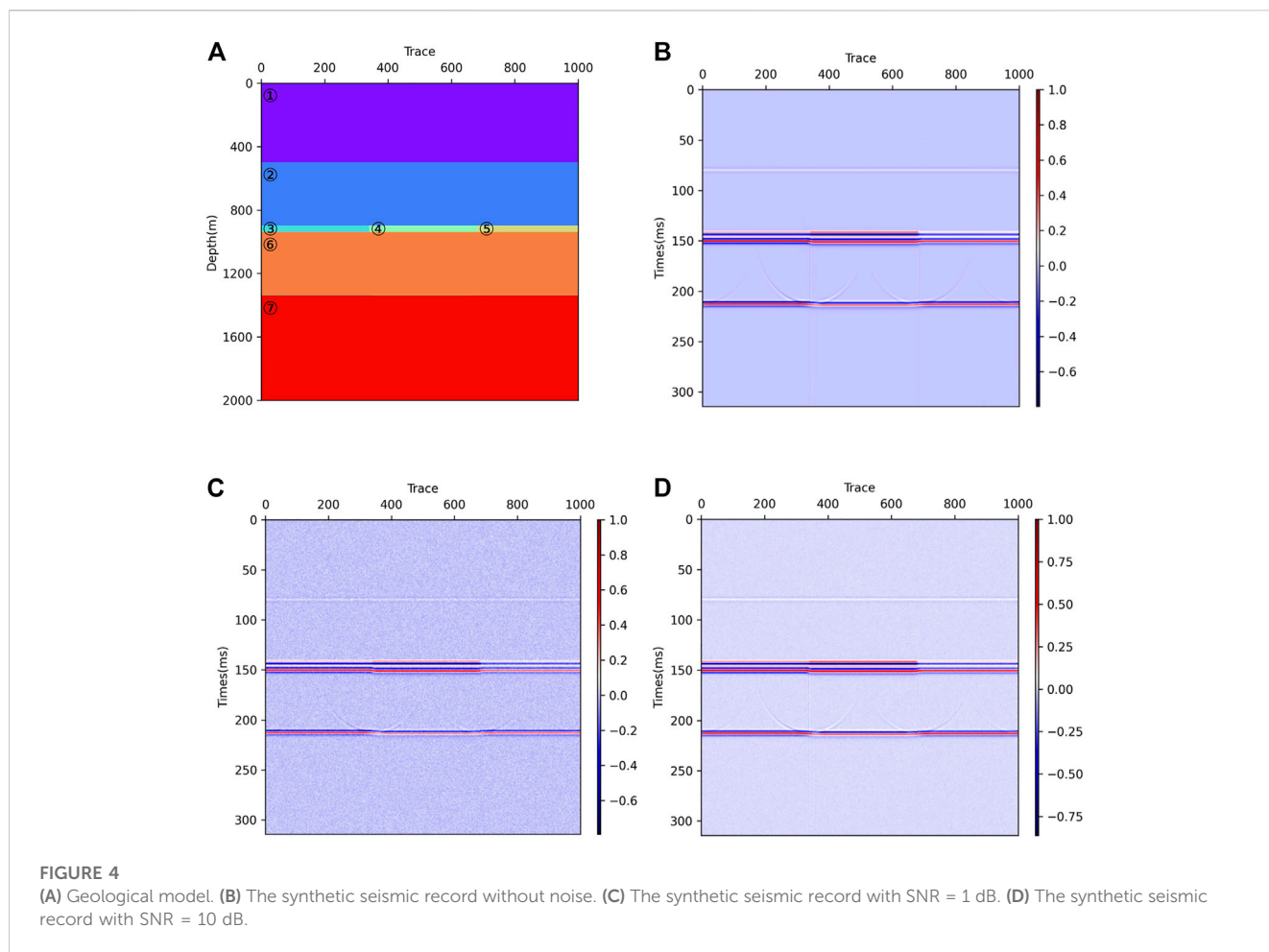
$$Cos(EM_g, EM_p) = 0.5 \times \frac{EM_g \cdot EM_p}{\|EM_g\| \cdot \|EM_p\|} + 0.5 \tag{4}$$

## 3 The experiment of the geological model

A geological attenuation model was developed to test the effectiveness of gas-bearing prediction with the dispersive viscosity equation (He et al., 2009). By referring to reservoir logging parameters and geological data in the Sichuan Basin, China, the geological model was designed and its parameters were configured in Table 1. In Figure 4A, Layer ③, ④, and ⑤ are the water-bearing reservoir, the gas-bearing reservoir, and the gas-water mixed reservoir, respectively, and they are all 40 m thick. The Ricker wavelet with a frequency of 30 Hz is employed to imitate seismic records, and the digital sampling frequency is 500 Hz. The model is first orthorectified based on the viscous dispersive wave equation, and then the simulated seismic profile was obtained by applying conventional wave equation offset. As a result, the synthetic seismic record is generated as shown in Figure 4B,

**TABLE 1** Rock properties for the geological model (where,  $V_p$  is the primary velocity,  $\rho$  is the density,  $\xi$  is the dispersion coefficient,  $\eta$  is the viscosity coefficient,  $Q$  is the attenuation coefficient).

Layer number	$V_p$ (m.s <sup>-1</sup> )	$\rho$ (g.cm <sup>-3</sup> )	$\xi$ (HZ)	$\eta$ (m <sup>2</sup> .s <sup>-1</sup> )	$Q$
①	6,246	2.7290	1	1	200
②	6,109	2.6850	1	1	200
③	6,400	2.7800	30	3	15
④	5,900	2.7280	10	500	5
⑤	5,950	2.7605	20	200	8
⑥	6,422	2.7256	1	1	200
⑦	6,426	2.8364	1	1	200



which is without noise. A particular amount of Gaussian white noise is added to the seismic record to imitate the low signal-to-noise (SNR) environment of the deeply underground reservoir. The SNR of the synthetic seismic record after adding noise ranges from 1 dB to 10 dB. **Figures 4C, D** show the synthetic seismic data at SNR = 1 dB and SNR = 10dB, respectively.

When preparing the dataset, the seismic records including the stratigraphic response of layers ③, ④, and ⑤ are divided into the seismic response of the water-bearing reservoir, the gas-bearing

reservoir, and the gas-water mixed reservoir, respectively. Ten seismic records with stratigraphic responses around layers ③, ④, and ⑤ are eliminated to limit the impact of distinct stratigraphic borders. Among the stratigraphic responses of each type of reservoir, 60% and 10% of the seismic records are selected randomly as training datasets and validation datasets respectively, while the remaining 30% are test datasets. In pre-processing and feature extraction, the parameter values are all adopted by our prior experiment. The pre-emphasis coefficient is 0.93, the frame

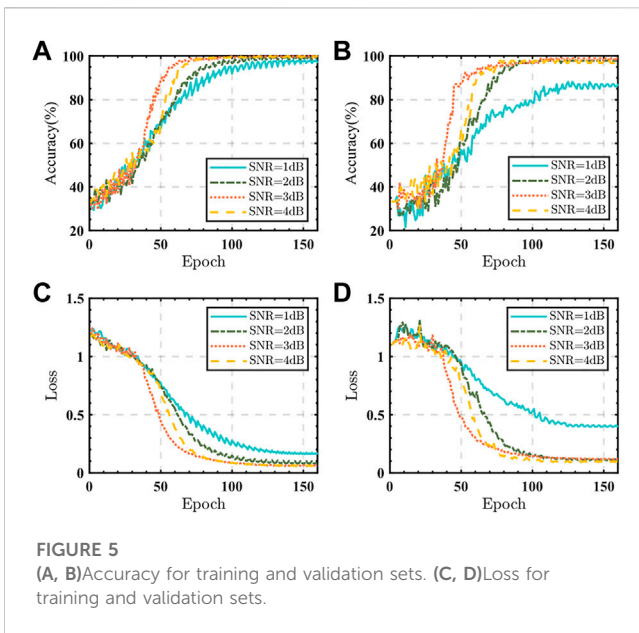


**FIGURE 5**  
(A, B) Accuracy for training and validation sets. (C, D) Loss for training and validation sets.

length is set to 20 milliseconds (ms), and the frameshift is set the half of the frame length. Besides, Hamming window is selected because the cepstrum coefficient calculated from it is relatively stable. Then, the seismic records' cepstrum parameters are calculated and fed into the DNN model. The DNN model in Kaldi is primarily written in C++, whereas the proposed DNN model is constructed and trained in Pytorch. When training a DNN model, the objective function is a multiclassification cross-entropy function, the optimizer uses Adam

(Barakat and Bianchi, 2021), and the learning strategy is OneCycle (Smith, 2017). The training process at extremely low SNR (1 dB~4 dB) is represented in Figure 5, while the training results with SNR greater than 4 dB are not shown since the accuracy of the training and validation datasets exceeds 98% and the loss is less than 0.1.

When the training of the DNN model is completed, the parameter values of each DNN layer are fixed. The embedding extracted from the seismic records at the center of layers ③, ④, and ⑤ is regarded as the embedding of reservoirs in which they are located. The cosine distance between the embedding of the seismic record to be predicted and three types of reservoir embedding is calculated respectively, and the reservoir corresponding to the highest cosine distance is the predicted reservoir. When the DNN input features are Cepstrum, MFCC, and FBank, three alternative gas-bearing prediction models are generated. From the result indicated in Figures 6A, B, it can be seen that cepstrum as a feature parameter has a robust advantage over the other two features.

The bottom layer of the x-vector uses TDNN with context to learn the segment feature in speech recognition. The effective response time of the reservoir in the seismic record is shorter than that of the speech record, and a shorter context should be set. In order to assess the impact of contextual width, we configure the TDNN-based gas-bearing prediction models with three time-delay strategies. These three strategies, labeled as TDNN\_311, TDNN\_331, and TDNN\_333, set the context of frames 1, frame 1~2, and frames 1~3 to 3 respectively, while the other layers have no delay. TDNN is implemented in the deep learning toolkit Torch by 1d-CNN because TDNN is equivalent to 1d-CNN (Daniel et al., 2018). Because the process of selecting the optimal

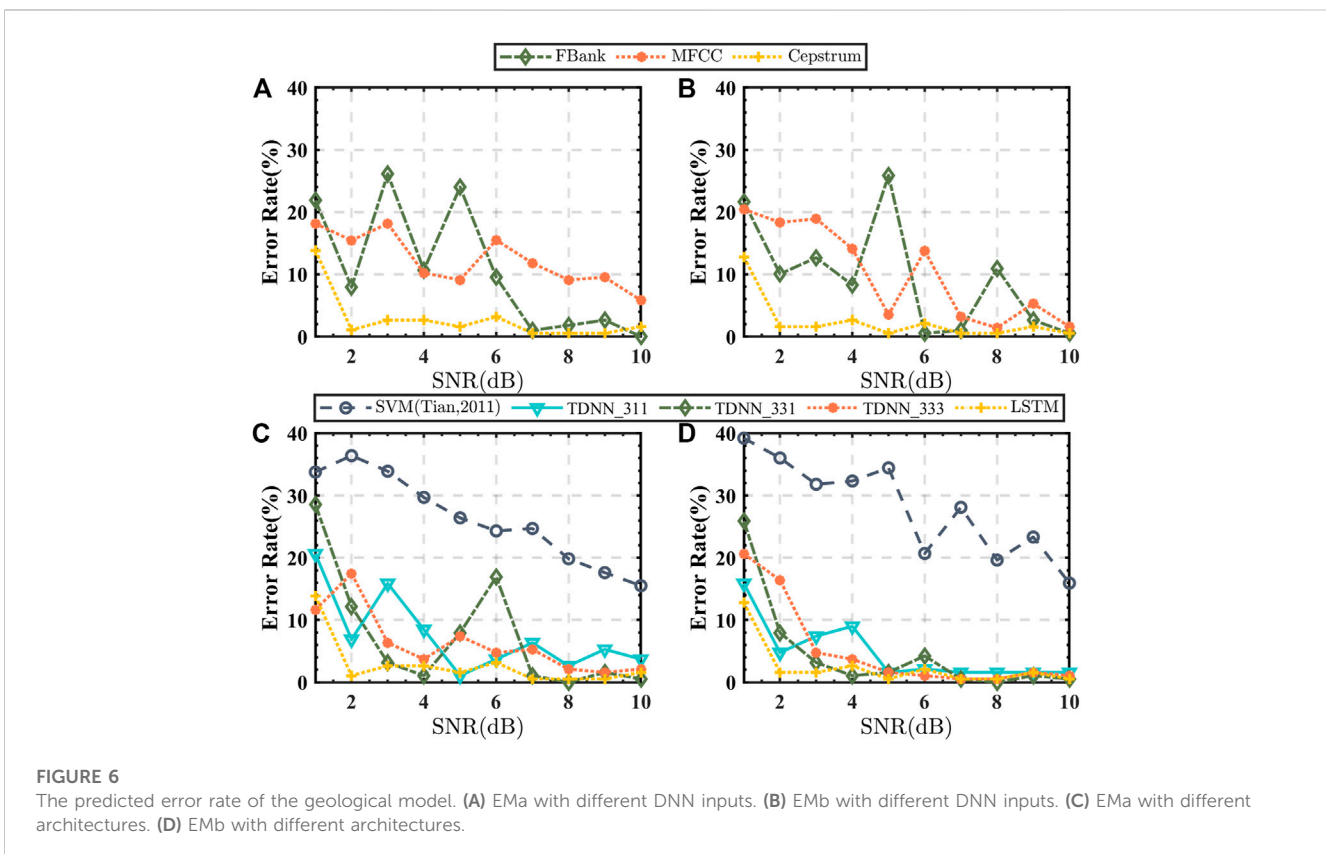


**FIGURE 6**  
The predicted error rate of the geological model. (A) EMA with different DNN inputs. (B) EMB with different DNN inputs. (C) EMA with different architectures. (D) EMB with different architectures.

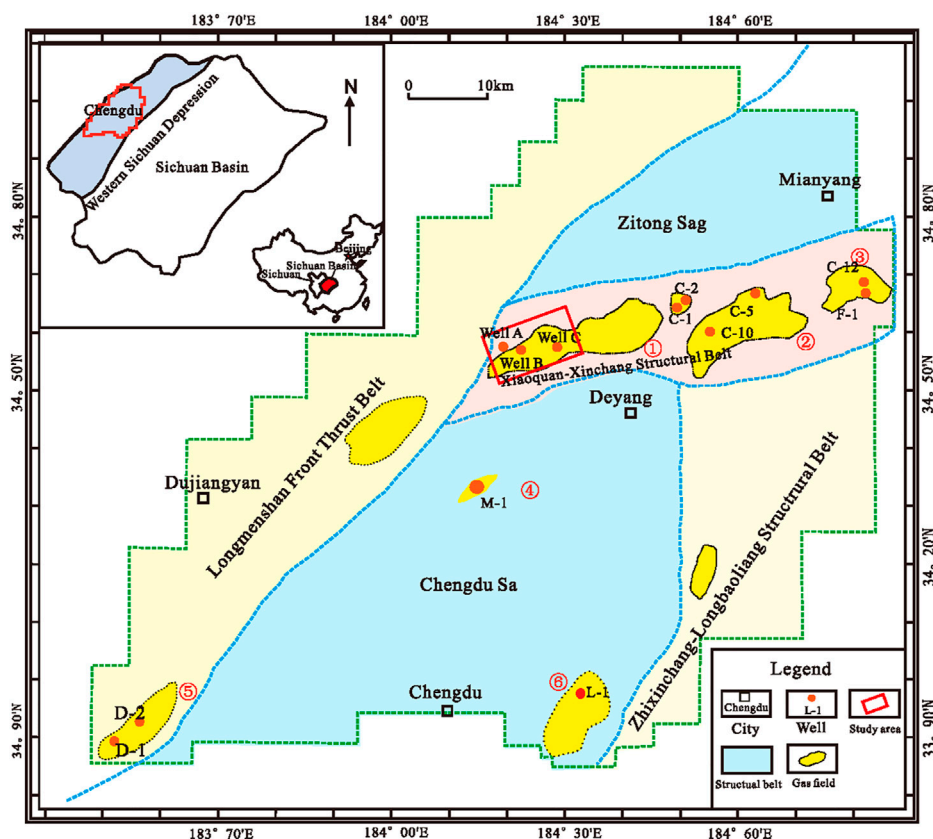


FIGURE 7 Structural diagram of the study area Cao et al. (2022).

combination from the three schemes is somewhat inefficient, we propose to replace TDNN with LSTM. To compare the improvement of the proposed method, we also compare it with previous studies (Tian and Cao, 2011), in which the absolute value of the difference between 1 and 2-order cepstral coefficients is extracted as the training samples of the support vector machine (SVM) classifier. The predicted error rate of the test samples belonging to the corresponding reserve is calculated based on different architectures respectively, which is shown in Figures 6C, D. The superior performance of LSTM shows that it may automatically learn the long-term relationships among sequences with the use of input gates, forgetting gates, output gates, and internal memory units.

### 4 The experiment of field

The work area is located in the Xiaoquan–Xinchang tectonic belt of the western Sichuan exploration area in China, with 150 km<sup>2</sup> as shown in Figure 7. This tectonic zone is mainly zonal distribution located in the Longmenshan foreland basin, one of the most important China’s natural gas-rich areas. The marine strata of this area dominated by carbonate is buried deep (about 4,000 m–7,000 m) including from Sinian to Middle Triassic. In this area, the Upper Triassic Maan Tang Formation (*T<sub>3m</sub>*) and the Leikoupo Formation (*T<sub>2l</sub>*) are the target layer due to massive

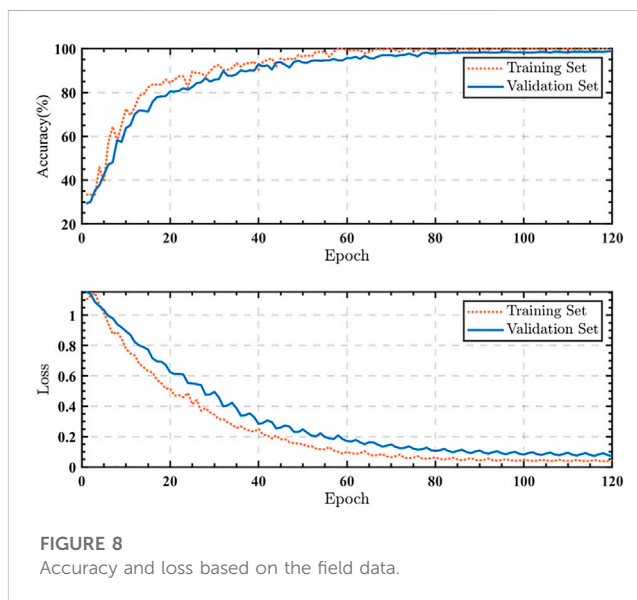
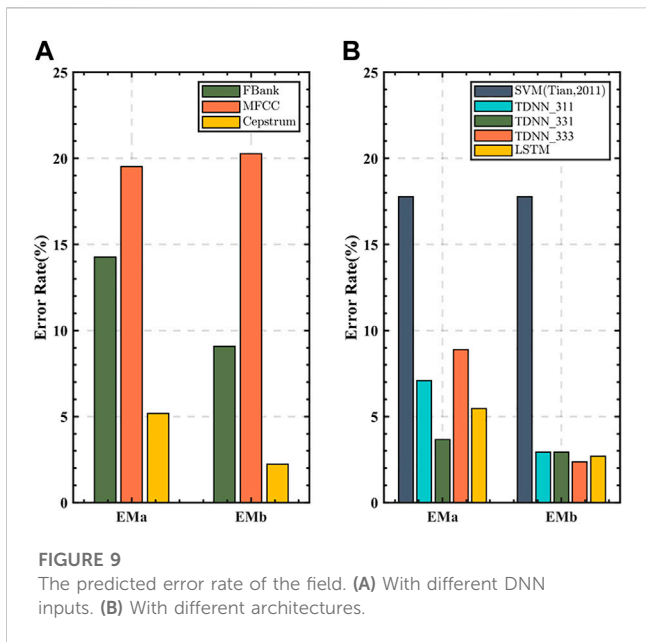


FIGURE 8 Accuracy and loss based on the field data.

natural gas resources. The thickness of the gas reservoir is thin, which results in minor differences in the physical parameters of the gas-bearing layer and surrounding rocks, and the poor seismic response signal makes exploration with current technologies



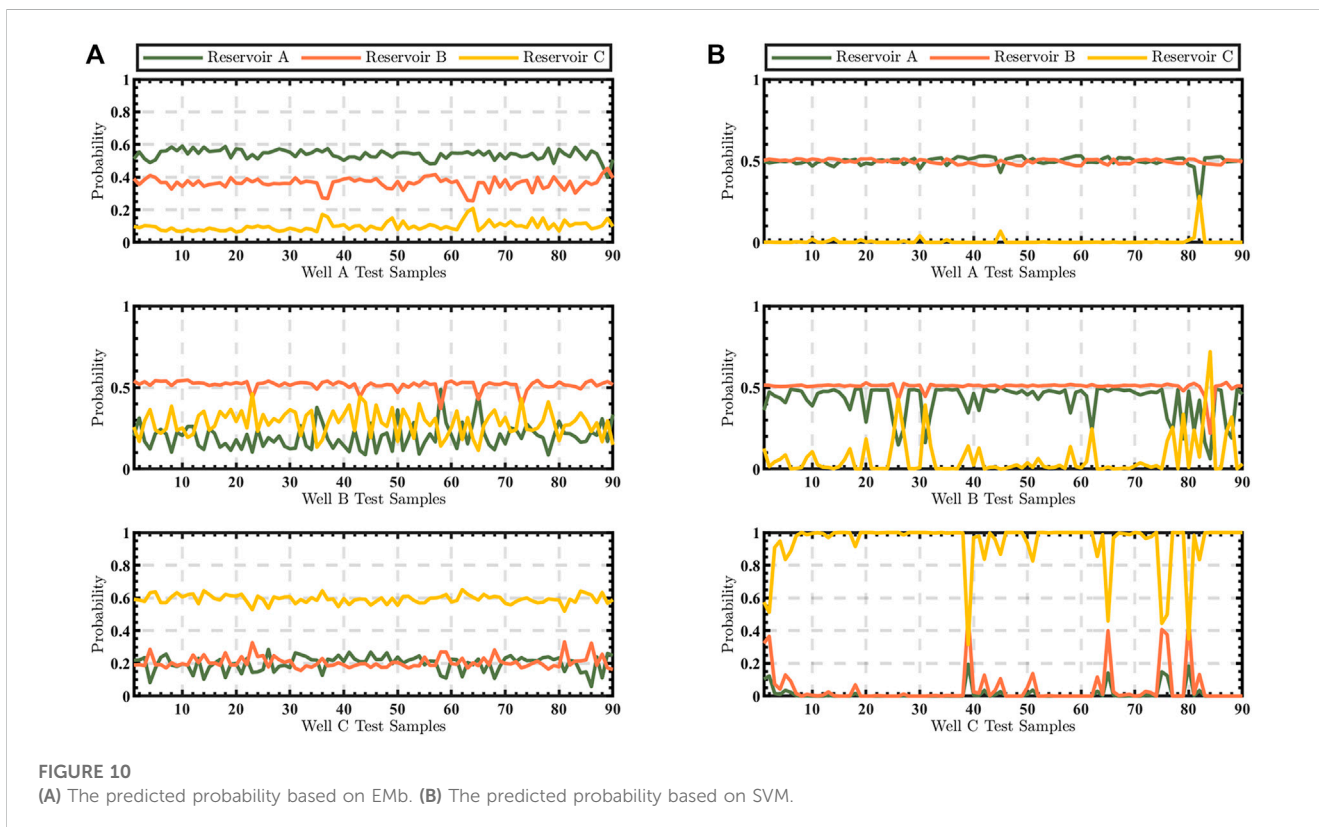
more difficult. There are three drilled well sites in the field area, and the geological formations of Well A, Well B, and Well C are a water-bearing reservoir, a gas-bearing reservoir, and a gas-water mixed reservoir in the target layer, respectively. When the datasets are generated, the seismic record from the top weathered crust of  $T_3m$  to the bottom of  $T_2l_4$  (around 150 m) is intercepted as the target layer along longitudinal time. Moreover, the seismic data (about

450 records) in the lateral 300 m range around Well A, B, and C is chosen. The seismic records close to the three wells are divided into three distinct types of stratigraphic response, namely, the seismic response of the water-bearing layer, the gas-bearing layer, and the gas-water mixed layer. The training and the validation curve are represented in Figure 8.

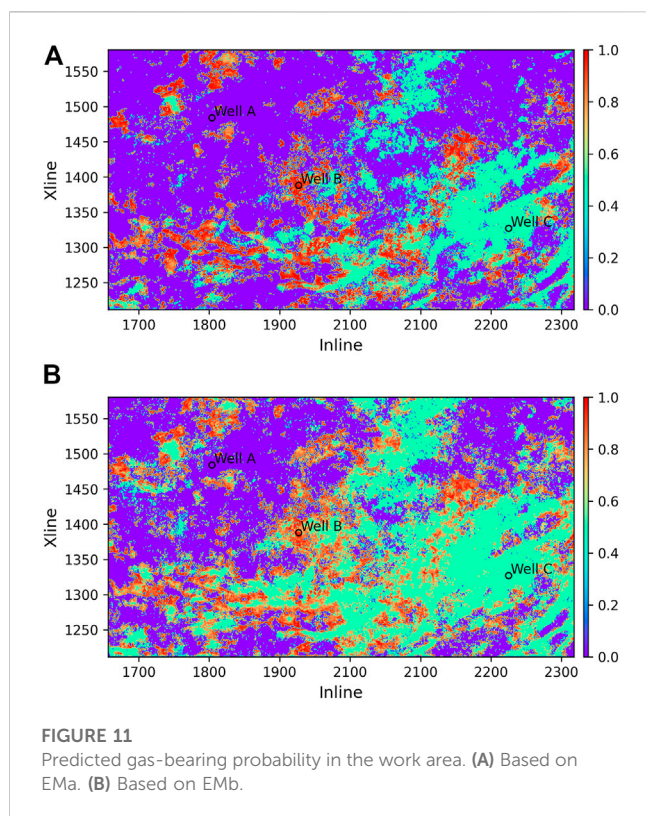
After training, the seismic embeddings nearest to three wells are generated and used as the reservoir represent in which they are located. The cosine distances are calculated independently by the embeddings of the to-be-predicted seismic records and the embeddings of three reservoirs. Subsequently, the cosine score with the gas reservoir indicates the gas-bearing probability. When the Cepstrum, MFCC, and FBank are selected as input features, it shows the same phenomenon in the geological model that the error rate with Cepstrum is lower than that of the other two feature parameters in Figure 9A. Similarly, Figure 9B shows that LSTM has a moderate performance compared with the three strategies of TDNN and obvious advantages over previous SVM architectures. Further, we list the probabilities of the test samples belonging to each category with the proposed and the previous method in Figure 10. To make the comparison fairer, we normalized each probability using the formula below, where  $j = 1, 2, 3$  denote the three categories of reservoirs, respectively,  $P_j$  is the initial probability, and  $\hat{P}_j$  is the normalized probability.

$$\hat{P}_j = \frac{P_j}{\sum_{i=1}^3 P_i}, j = 1, 2, 3 \quad (5)$$

To visualize the gas-bearing distribution clearly, the proposed approach is applied to the whole work area. In Figure 11, the value of







the region predicted as reservoir B is equal to the cosine scoring, whereas the value of the region predicted to be reservoir A and C are set to 0 and 0.5, respectively. The prediction results based on the two embeddings show comparable gas-bearing distribution zones, while the gas-bearing region based on Emb is slightly larger which is consistent with the result in Figure 9 that fewer of the gas-bearing test samples are poorly predicted.

## 5 Conclusion

To deal with the difficult challenge of gas-bearing prediction in deeply buried reservoirs, this paper proposes an innovative gas-bearing prediction model based on DNN embedding. Motivated by the similarity between seismic data and acoustic data, the DNN model is designed by referring to the structure of the x-vector in speech identification, in which gas-sensitive cepstral parameters are the input, the bottom layers are LSTM networks that can learn the contextual relationship of the seismic waveforms, and the output is a DNN embedding used for similarity scoring. The validity of the proposed method was demonstrated in both generated synthetic seismic records and actual seismic data. The next study is to consider

## References

- Barakat, A., and Bianchi, P. (2021). Convergence and dynamical behavior of the adam algorithm for nonconvex stochastic optimization. *Siam J. Optim.* 31 (1), 244–274. doi:10.1137/19m1263443
- Cao, J., Jiang, X., Xue, Y., Tian, R., Xiang, T., and Cheng, M. (2022). The state-of-the-art techniques of hydrocarbon detection and its application in ultra-deep carbonate

the hyperparametric assessment since the parameters in feature extraction and DNN training are mainly chosen empirically. Furthermore, data augmentation might be explored to improve predictive capabilities because data amount is the fundamental restriction of DNN.

## Data availability statement

The original contributions presented in the study are included in the article/Supplementary Material, further inquiries can be directed to the corresponding author.

## Author contributions

All authors listed have made a substantial, direct, and intellectual contribution to the work and approved it for publication.

## Funding

The authors declare that this study received funding from the project of the SINOPEC Science and Technology Department (Grant No. P20055-6). The funder was not involved in the study design, collection, analysis, interpretation of data, the writing of this article, or the decision to submit it for publication.

This work was supported by the National Natural Science Foundation of China (Grant Nos. 42030812 and 41974160), Chengdu University of Technology Postgraduate Innovative Cultivation Program (Grant No. CDUT2022BJCX009), Technological Development for Sichuan Province (2021ZYD0030), and Natural Science Foundation of Sichuan (No. 2023NSFSC0258).

## Conflict of interest

The authors declare that the research was conducted in the absence of any commercial or financial relationships that could be construed as a potential conflict of interest.

## Publisher's note

All claims expressed in this article are solely those of the authors and do not necessarily represent those of their affiliated organizations, or those of the publisher, the editors and the reviewers. Any product that may be evaluated in this article, or claim that may be made by its manufacturer, is not guaranteed or endorsed by the publisher.

reservoir characterization in the Sichuan Basin, China. *Front. Earth Sci.* 10. doi:10.3389/feart.2022.851828

Cao, J., Liu, S., Tian, R., Wang, X., and He, X. (2011). Seismic prediction of carbonate reservoirs in the deep of Longmenshan foreland basin. *Acta Petrol. Sin.* 27 (8), 2423–2434.

- Cao, J., Xue, Y., Tian, R., and Shu, Y. (2019). Advances in hydrocarbon detection in deep carbonate reservoirs. *Geophys. Prospect. Petroleum* 58 (1), 9–16.
- Coléou, T., Poupon, M., and Azbel, K. (2003). Unsupervised seismic facies classification: A review and comparison of techniques and implementation. *Lead. Edge* 22 (10), 942–953. doi:10.1190/1.1623635
- Daniel, P., Cheng, G., Yiming, W., Li, K., Xu, H., Yarmohamadi, M., et al. (2018). “Semi-orthogonal low-rank matrix factorization for deep neural networks,” in Proceedings of the Conference of the International Speech Communication Association (INTERSPEECH), Hyderabad, India, September 2018.
- Gao, J., Song, Z., Gui, J., and Yuan, S. (2022). Gas-bearing prediction using transfer learning and CNNs: An application to a deep tight dolomite reservoir. *Ieee Geoscience Remote Sens. Lett.* 19, 1–5. doi:10.1109/lgrs.2020.3035568
- Hall, M. (2006). Predicting bed thickness with cepstral decomposition. *Lead. Edge* 25(2)199–204.
- Hammond, A. L. (1974). Bright spot: Better seismological indicators of gas and oil. *Science* 185 (4150), 515–517. doi:10.1126/science.185.4150.515
- Hampson, D. (1991). AVO inversion, theory and practice. *Lead. Edge* 10 (6), 39–42. doi:10.1190/1.1436820
- He, Z., Xiong, X., and Bian, L. (2009). Numerical simulation of seismic low-frequency shadows and its application. *Appl. Geophys.* 5 (4), 301–306. doi:10.1007/s11770-008-0040-4
- Kumar, M., Jin-Park, T., Bishop, S., and Narayanan, S. (2020). Designing neural speaker embeddings with meta learning. <https://arxiv.org/abs/2007.16196>.
- Liu, D., Wang, X., Yang, X., Mao, H., Sacchi, M. D., and Chen, W. (2022). Accelerating seismic scattered noise attenuation in offset-vector tile domain: Application of deep learning. *Geophysics* 87 (5), 505–519. doi:10.1190/geo2021-0654.1
- Liao, X., Cao, J., Hu, J., You, J., Jiang, X., and Liu, Z. (2020). First arrival time identification using transfer learning with continuous wavelet transform feature images. *Ieee Geoscience Remote Sens. Lett.* 17 (11), 2002–2006. doi:10.1109/lgrs.2019.2955950
- Liu, D., Wang, W., Wang, X., Wang, C., Pei, J., and Chen, W. (2020). Poststack seismic data denoising based on 3-D convolutional neural network. *Ieee Trans. Geoscience Remote Sens.* 58 (3), 1598–1629. doi:10.1109/tgrs.2019.2947149
- Liu, Z., Cao, J., You, J., Chen, S., Lu, Y., and Zhou, P. (2021). A lithological sequence classification method with well log via SVM-assisted bi-directional GRU-CRF neural network. *J. Petroleum Sci. Eng.* 205, 108913. doi:10.1016/j.petrol.2021.108913
- Muda, L., Begam, M., and Elamvazuthi, I. (2010). Voice recognition algorithms using Mel frequency cepstral coefficient (MFCC) and dynamic time warping (DTW) techniques. <https://arxiv.org/abs/1003.4083>.
- Qu, X., Yan, G., Zheng, D., Fan, S., Rao, Q., and Jiang, J. (2021). A deep learning-based automatic first-arrival picking method for ultrasound sound-speed tomography. *Ieee Trans. Ultrason. Ferroelectr. Freq. Control* 68 (8), 2675–2686. doi:10.1109/TUFFC.2021.3074983
- Smith, L. N. (2017). “Cyclical learning rates for training neural networks,” in Proceedings of the 17th IEEE Winter Conference on Applications of Computer Vision (WACV), Waikoloa, HI, USA, January 2017, 464–472.
- Snyder, D., Garcia-Romero, D., Povey, D., and Khudanpur, S. (2017). “Deep neural network embeddings for text-independent speaker verification,” in Proceedings of the Conference of the International Speech Communication Association, Stockholm, Sweden, August 2017.
- Snyder, D., Garcia-Romero, D., Sell, G., Povey, D., and Khudanpur, S. (2018). “X-Vectors: Robust DNN embeddings for speaker recognition,” in Proceedings of the 2018 IEEE International Conference on Acoustics, Speech and Signal Processing (ICASSP), Calgary, Canada, April 2018.
- Song, Z., Li, S., He, S., Yuan, S., and Wang, S. (2022). Gas-bearing prediction of tight sandstone reservoir using semi-supervised learning and transfer learning. *Ieee Geoscience Remote Sens. Lett.* 19, 1–5. doi:10.1109/lgrs.2022.3177314
- Taner, M. T., Koehler, F., and Sheriff, R. E. (1979). Complex seismic trace analysis. *Geophysics* 44 (6), 1041–1063. doi:10.1190/1.1440994
- Tian, R.-F., and Cao, J.-X. (2011). “Application of support vector machine method for predicting hydrocarbon in the reservoir,” in Proceedings of the 2011 International Conference on Computational and Information Sciences, Washington, DC, USA, October 2011.
- Tschannen, V., Delescluse, M., Ettrich, N., and Keuper, J. (2020). “Extracting horizon surfaces from 3D seismic data using deep learning,” N17–N26. doi:10.1190/geo2019-0569.1*Geophysics*853
- Wang, F., and Chen, S. (2019). Residual learning of deep convolutional neural network for seismic random noise attenuation. *Ieee Geoscience Remote Sens. Lett.* 16 (8), 1314–1318. doi:10.1109/lgrs.2019.2895702
- Wang, J., Li, L., Wang, D., and Zheng, T. F. (2014). “Research on generalization property of time-varying fbank-weighted MFCC for I-vector based speaker verification,” in Proceedings of the 9th International Symposium on Chinese Spoken Language Processing 2014, Singapore, September 2014.
- Xie, T., Zheng, X.-D., and Zhang, Y. (2016). Seismic facies analysis based on linear prediction cepstrum coefficients. *Chin. J. Geophysics-Chinese Ed.* 59 (11), 4266–4277. doi:10.6038/cjg20161127
- Xie, T., Zheng, X., and Zhang, Y. (2017). Seismic facies analysis based on speech recognition feature parameters. *Geophysics* 82 (3), O23–O35. doi:10.1190/geo2016-0121.1
- Xue, Y., Cao, J., Tian, R., Du, H., and Yao, Y. (2016). Wavelet-based cepstrum decomposition of seismic data and its application in hydrocarbon detection. *Geophys. Prospect.* 64 (6), 1441–1453. doi:10.1111/1365-2478.12344
- Yang, J., Lin, N., Zhang, K., Zhang, C., Fu, C., Tian, G., et al. (2021). Reservoir characterization using multi-component seismic data in a novel hybrid model based on clustering and deep neural network. *Nat. Resour. Res.* 30 (5), 3429–3454. doi:10.1007/s11053-021-09863-z
- Zhang, K., Lin, N.-T., Yang, J.-Q., Jin, Z.-W., Li, G.-H., and Ding, R.-W. (2022). Predicting gas-bearing distribution using DNN based on multi-component seismic data: Quality evaluation using structural and fracture factors. *Petroleum Sci.* 19 (4), 1566–1581. doi:10.1016/j.petsci.2022.02.008
- Zheng, F., Zhang, G. L., and Song, Z. J. (2001). Comparison of different implementations of MFCC. *J. Comput. Sci. Technol.* 16 (6), 582–589. doi:10.1007/bf02943243